**Jurnal Asiimetrik: Jurnal Ilmiah Rekayasa Dan Inovasi**
Accredited "**SINTA 3**" based on the Decree of Dirjendiktiristek, Number: 225/E/KPT/2022
Volume 7 Number 1, January 2025, Page 71-82
Website : http://journal.univpancasila.ac.id/index.php/asiimetrik/

*p-ISSN 2655-1861*
*e-ISSN 2716-2923*

# The Effect of Hydrostatic Pressure on the Performance of Oscillating Wave Surge Converter

## Pengaruh Tekanan Hidrostatis Terhadap Performa *Oscillating Wave Surge Converter*

**Anton Dwi Prabowo[1], James Julian[1*], Fitri Wahyuni[1], Riki Hendra Purba[1], Nely Toding Bunga[2]**
[1]Department of Mechanical Engineering, Faculty of Engineering, Universitas Pembangunan Nasional Veteran Jakarta, Jawa Barat, Indonesia
[2]Department of Mechanical Engineering, Faculty of Engineering, Universitas Pancasila, Jakarta, Indonesia

**Article information:**

Received:
09/12/2024
Revised:
18/12/2024
Accepted:
19/12/2024

### Abstract

The latest energy demand increasingly drives innovation in ocean wave energy technology, including the Oscillating Wave Surge Converter (OWSC). This consider analyzes the impact of water profundity varieties on the execution of OWSCs put on the seabed. The study was conducted numerically using the Boundary Element Method by testing four variations of air depth at wave periods between 1.2 and 2.8 seconds and wave amplitudes of 0.1 meters. The results show that the optimal depth, equivalent to the flap height (D2), produces the highest maximum displacement due to the balance between hydrostatic pressure and wave energy the flap receives. Conversely, depths that are too shallow (D1) or too deep (D4) result in smaller displacements due to the instability of the movement in shallow air and the attenuation of wave energy in deep air. In addition, more extended wave periods tend to decrease the changing cycle frequency but increase the symmetry of the flap movement at a certain depth.

***Keywords:*** oscillating wave surge converter, depth, Boundary Element Method.

***SDGs*:**


### Abstrak

Permintaan akan energi terbarukan mendorong pengembangan teknologi energi gelombang laut, termasuk *Oscillating Wave Surge Converter* (OWSC). Penelitian ini bertujuan untuk menginvestigasi pengaruh variasi kedalaman air terhadap kinerja perangkat OWSC yang dipasang di dasar laut. Variasi kedalaman diuji pada 4 kedalaman yang berbeda dengan menggunakan metode numerik berbasis *Boundary Element Method* pada periode gelombang antara 1,2 detik hingga 2,8 detik dengan amplitudo gelombang 0,1 meter. Hasil penelitian menunjukkan bahwa kedalaman yang setara dengan tinggi *flap* (D2), menghasilkan *displacement* maksimum tertinggi akibat keseimbangan antara tekanan hidrostatis dan energi gelombang yang diterima *flap*. Kedalaman yang terlalu dangkal (D1) atau terlalu dalam (D4) menghasilkan *displacement* yang lebih kecil, disebabkan oleh ketidakstabilan gerakan pada kedalaman dangkal dan redaman energi pada kedalaman yang lebih dalam. Selain itu, peningkatan periode gelombang menyebabkan penurunan frekuensi siklus *displacement*, namun meningkatkan simetri gerakan flap pada kedalaman tertentu.

***Kata Kunci:*** *oscillating wave surge converter*, kedalaman, *Boundary Element Method*.

*Correspondence Author
email : zames@upnvj.ac.id

## 1. INTRODUCTION

The demand for renewable energy has driven the exploration of energy processing from the marine sector. Ocean wave energy is one form of renewable energy that comes from the ocean (Constant *et al.*, 2021). Innovations related to renewable energy that utilize ocean wave energy are Wave Energy Converters (WEC). The application of WEC is categorized into several types, namely, Oscillating Water Columns, Wave Activated Bodies, and Oscillating Wave Surge Converter (Bertram *et al.*, 2020). Of the various types of WEC, there is another classification regarding the location of the device application: on shore, near shore, and offshore (Bertram *et al.*, 2020). In general, the further offshore the ocean wave energy will be more incredible, but the manufacturing and maintenance costs will be more significant. Nearshore is the most effective location for utilizing ocean wave energy. The type of WEC whose application is located nearshore is the Oscillating Wave Surge Converter (OWSC). Specifically, OWSC is a device that utilizes kinetic energy from ocean waves to be converted into mechanical energy through a plate structure (Flap) applied to the seabed (Gunawardane, Folley and Kankanamge, 2019). Then, this mechanical energy will be converted into electrical energy as an alternative to ocean wave energy.

Researchers have widely discussed the development of OWSC devices. A study investigated the hydrodynamic characteristics of OWSC devices against sea waves. The method used in this study is a numerical approach that varies the sea wave period. The results of this study are changes in the motion response of the OWSC device influenced by its wave period (Julian *et al.*, 2024). This study's exploration is limited to hydrodynamic characteristics, so many parameters have yet to be considered to review the performance of the OWSC. One parameter that affects the performance of the device is the shape of the flap structure. This body was investigated in another study by varying the shape of the flap into a cylinder and a rectangle. The variation in geometry was tested at different water depths but at most the height of the flap. The results of this study show that the OWSC device with a rectangular flap geometry can capture more energy than the cylindrical geometry. In addition, the performance of the OWSC device will increase at shorter water depths (Cui, Chen and Dai, 2023). It means that in addition to geometry, depth also affects the performance of the OWSC. However, the depth variation in this study is only limited to the height of the flap, and further discussion has yet to be held on when the OWSC device is placed in deeper seas. Another study discusses the OWSC device with a floating configuration. This study tested the device at water depths of 0.47 m, 1 m, 2 m, and 3 m. The findings revealed that shallower water depths enhance device efficiency by up to 55%, attributed to the shoaling effect in shallow sea conditions (Cheng *et al.*, 2020). The understanding of the influence of water depth has been well explained in this study, but the discussion related to the condition of the device placed on the seabed has yet to be explained. Other studies discuss the device's application in tiered sea topography conditions. This study shows that a quarter wavelength resonance above tiered sea topography will increase the hydrodynamic efficiency of the device. In this study, the condition of water depth has yet to be explained in more depth, so a study is needed on the variation of sea depth on OWSC performance (Zhang, Zhu and Cheng, 2023).

While various studies have explored the performance of Oscillating Wave Surge Converters (OWSC) under different configurations, such as variations in flap geometry, water depth, and floating applications, certain aspects remain less understood. Specifically, the interaction between OWSC devices placed on the seabed and the varying conditions of seawater depth has received limited attention. Challenges such as hydrostatic pressure and its influence on device efficiency and structural integrity have yet to be thoroughly investigated. This fact highlights the need for further research to optimize the deployment and performance of OWSC devices in seabed applications under diverse depth conditions. This study specifically focuses on examining the impact of seawater depth on the condition of devices positioned on the seabed. Hopefully, this

study can be a reference for consideration in the optimal placement of OWSC devices.

## 2. METHODOLOGY

### 2.1. Ocean Wave Properties

The WEC device needs to absorb energy from ocean waves as a power source to generate electricity. Ocean waves are generated from an initial condition that is balanced, then affected by external forces (wind or vibrations), after which a restoring force appears that tries to reverse the condition to balance. Finally, the process causes waves to continue to move. The process of ocean wave movement that heads to the beach will experience a change in shape (Toffoli and Bitner-Gregersen, 2017). The movement pattern of ocean waves will be circular along with the water current. Then, the ocean wave particles that were initially circular will change into ellipses when the sea water becomes shallower (Garrison and Ellis, 2022). This phenomenon causes ocean waves to have three categories: shallow ocean waves, transitional ocean waves, and deep ocean waves (see Figure 1).

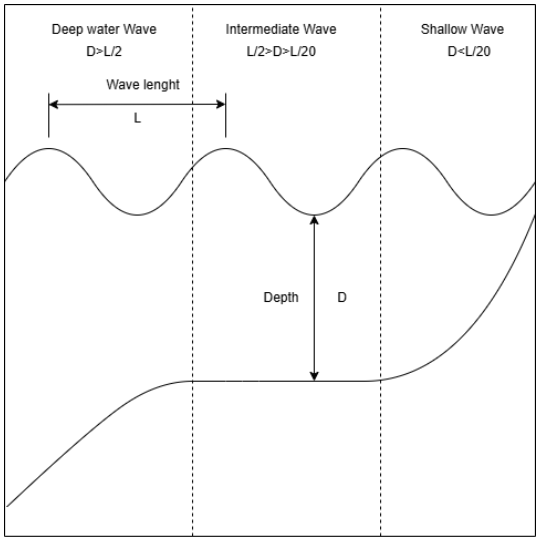


**Figure 1.** Wave characterization.

Shallow ocean waves occur when the depth of the seawater is less than or equal to l/20. In this condition, the seabed will affect water movement. Then, the condition of the transition wave is when the water depth is between l/2 and l/20. Generally, this condition occurs between the deep sea and offshore. The final deep ocean wave occurs when the depth of the seawater exceeds half the wavelength. In this condition, the waves will not feel the influence of the seabed. Generally, WEC devices will be applied in onshore areas with shallow wave types, near-shore with transitional wave types, and offshore with deep wave types (Wilberforce *et al.*, 2019). This study will investigate the OWSC device in near-shore areas with transitional sea wave conditions so that the effect of water depth on OWSC performance can be known.

### 2.2. Setup Geometry

OWSC is a device that utilizes the kinetic energy of ocean waves absorbed by the flap structure, where the movement of this flap will be like an inverted pendulum that produces mechanical force and will be converted into electricity (Cheng *et al.*, 2021). Figure 2 presents an isometric view of OWSC. This study used the OWSC model studied by Wei et al., with a scale down up to 40 times from the experimental dimensions (Wei *et al.*, 2016). Specifically, the test parameters used in this study are described in Table 1.

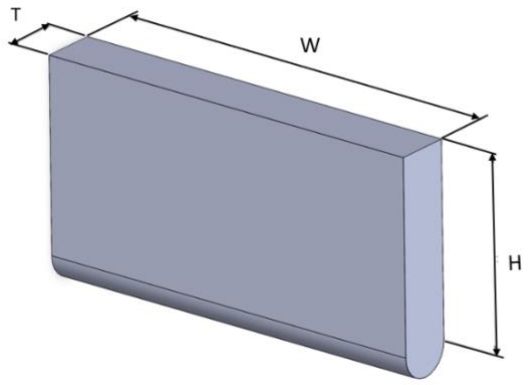


**Figure 2.** Isometric view.

This study analyzed the effect of seawater depth, and the water depth varied at different levels, as explained in Table 2. Furthermore, to model the boundary conditions of ocean waves as in Wei's research, this study varies the wave period from 1.2 s to 2.8 s, as shown in Table 3. ensuring that measurements comprehensively cover representative wave conditions (Wei *et al.*, 2016).

**Table 1.** Test parameters.

| No. | Parameters | Value |
|---|---|---|
| 1 | Scalling factor | 1 : 40 |
| 2 | W (m) | 0.646 |
| 3 | H (m) | 0.35375 |
| 4 | T (m) | 0.0875 |
| 5 | Mass (kg) | 4.7 |

**Table 2.** Depth variations.

| No. | Parameters | Value |
|---|---|---|
| 1 | D1 (m) | 0.5 H |
| 2 | D2 (m) | 1 H |
| 3 | D3 (m) | 1.5 H |
| 4 | D4 (m) | 2 H |

**Table 3.** Sea wave parameters.

| No. | Parameters | Value |
|---|---|---|
| 1 | 0.01 | 1.2 |
| 2 | 0.01 | 1.4 |
| 3 | 0.01 | 1.6 |
| 4 | 0.01 | 1.8 |
| 5 | 0.01 | 2 |
| 6 | 0.01 | 2.2 |
| 7 | 0.01 | 2.4 |
| 8 | 0.01 | 2.6 |
| 9 | 0.01 | 2.8 |
| 10 | 0.01 | 3 |
| 11 | 0.01 | 1.2 |

### 2.3. Boundary Element Method (BEM)

Numerical calculation methods evaluate the tests conducted and solve testing problems. The boundary element method defines the influence of sea waves with flap structures. Ansys Aqwa Hydrodynamics Diffraction is used to solve hydrodynamic problems, namely frequency and time domains. This study assumes that the fluid conditions have incompressible properties and inviscid flow. In this study, linear waves represent the phenomenon of sea waves, described through equation (1). Linear potential flow theory calculates the wave force acting on the OWSC. This theory is stated in equation (2) as the potential velocity of the flow field. In observing the performance of the OWSC, the entire system is represented by an equation (Tongphong *et al.*, 2021). Calculating nonlinear hydrostatic forces and Froude-Krylov wave forces using the time domain is used to solve the problem of motion response in the OWSC system, as shown in equation (3) (Rahman, 1995). Meanwhile, equation (4) describes the output of the motion response of the OWSC system in the form of a frequency domain.

$$\eta(x,t)=\frac{h}{2}\cos(\omega t-k(x\cos\theta)) \tag{1}$$

$$\nabla^2\phi(x,y,z,t)= \phi_I(x,y,z,t)+\phi_D(x,y,z,t)+ \phi_R(x,y,z,t)=a_W\varphi(x,y,z)e^{-i\omega t} \tag{2}$$

$$M\ddot{X}(t)+C\dot{X}(t)+KX(t)+C_h\dot{X}(t) =\sum F(t) \tag{3}$$

$$\left[-\omega^2(M_s+M_a(\omega))-i\omega C(\omega)+K\right] X(\omega)=F(\omega) \tag{4}$$

where:

$\eta(x,t)$ = Wave surface elevation at position and time (m)
$h$ = Wave amplitude (m)
$\omega$ = Angular frequency (rad/s)
$k$ = Wave number (rad/m)
$\theta$ = Angle of incidence of the wave (°)
$\phi_1$ = Wave velocity potential ($m^2/2$)
$\phi_D$ = Wave diffraction potential ($m^2/2$)
$\phi_R$ = Wave radiation potential ($m^2/2$)
$M$ = Mass matrix (kg)
$C$ = Damping matrix (kg/s)
$K$ = Structural stiffness matrix
$X$ = Motion response (°)
$F$ = Wave exciting force

### 2.4. Mesh Independent Test

The mesh-independent test is used to ensure the data quality in research using numerical methods. The mesh-independent test method used in this study is the Roache method (Roache, 1994). This study tested variations in fine, medium, and coarse mesh categories. The number of elements tested was 24629, 17643, and 11673.

As an example of testing, flap response oscillations were used for each mesh category and processed using the root mean square (RMS) shown in Equation (6). Each mesh category is identified by the mesh refinement ratio calculated by equation (7).

$$x_{RMS} = \sqrt{\frac{1}{n}\sum(x^2)} \quad (6)$$

where:

$x_{RMS}$ = Root Mean Square Displacement - a measure of the displacement's variability (°)

$$r = \frac{h_2}{h_1} \quad (7)$$

where:

r = Ratio between two grid sizes (dimensionless)

$$\overline{p} = \frac{\ln\left(\frac{f_3 - f_2}{f_2 - f_1}\right)}{\ln(r)} \quad (8)$$

where:

$\overline{p}$ = Convergence Order (dimensionless)

$$GCI_{fine} = \frac{F_s |\in|}{\left(r^{\overline{p}} - 1\right)} \quad (9)$$

where:

$GCI_{fine}$ = Grid Convergence Index for fine mesh (dimensionless)

$$GCI_{coarse} = \frac{F_s |\in| r^{\overline{p}}}{\left(r^{\overline{p}} - 1\right)} \quad (10)$$

where:

$GCI_{coarse}$ = Grid Convergence Index for coarse mesh (dimensionless)

$$f\,r_{h=0} = f_1 + \frac{(f_1 - f_2)}{\left(r^{\overline{p}} - 1\right)} \quad (11)$$

where:

$f\,r_{h=0}$ = Reference Solution for zero refinement (°)

Furthermore, the sequence value is determined using Equation (8). When testing the error value for each grid category, the grid convergence index (GCI) calculated by equations (9) and (10) is used as a parameter. GCI is divided into two categories. GCIfine is an error value between fine and medium mesh, and GCIcoarse is an error value between medium and coarse mesh. The GCI calculation must be in the convergence region to ensure that the error value of each network is correct. Therefore, the value of the network independence study can be found using Equation (11). The test was carried out on a water wave amplitude of 0.1 m with a wave period of 2 seconds and a depth of D2. The calculation results presented in the table showed that the fine mesh had guaranteed accuracy with the smallest error value. Therefore, the fine mesh was selected for the test mesh setting. **Table 4** showing the results of the mesh independence test.

**Table 4.** Mesh independence test results.

| Mesh | *Fine* | *Medium* | *Coarse* |
|---|---|---|---|
| *Respons* | 51.43305594 | 50.3015287 | 47.38404004 |
| *r* | | 1.292781749 | |
| $GCI_{fine}$ | | 1.782% | |
| $GCI_{coarse}$ | | 4.5934% | |
| $\frac{GCI_{coarse}}{GCI_{fine} r^{\overline{p}}}$ | | 1 | |
| *Error* | 1.37469% | 3.54444% | 9.13887% |

## 3. RESULTS AND DISCUSSION

### 3.1. Validation

In this study, the device displacement data produced by the Wei et al. experiment was used as a reference for comparison. The device was tested at a water wave amplitude of 0.1 and a water wave period of 1.9 s. The outcomes of the numerical method in this study closely resembled the experimental results obtained by Wei et al. (Wei *et al.*, 2016).

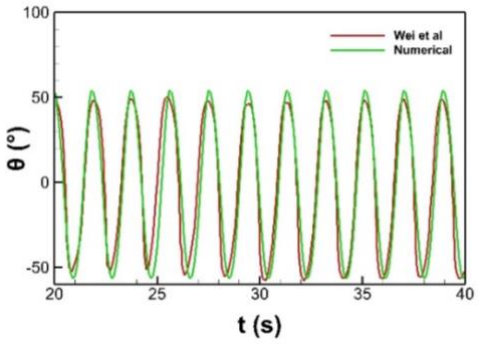


**Figure 3.** Validation data.

Figure 3 shows that the frequency of displacement movements obtained from the numerical calculations matches the magnitude observed in the experiment. Although there are differences in the results of the displacement cycle produced by the device, this similarity shows that the numerical calculation can display results that are close to the actual, thus increasing the validity of this study.

### 3.2. Analysis

This study focuses on the characteristics of the motion response that occurs in the OWSC device. In this study, test samples were taken at a sea wave amplitude of 0.1 m, and the wave period varied in the range of 1.2 s, 1.6 s, 2 s, 2.4 s, and 2.8 s. The results of the displacement comparison at the sea wave period T = 1.2 s are shown in Figure 4. The data presented shows that the movement produced by the device due to sea waves is a sinusoidal curve. If examined more deeply, it can be seen that depth will significantly affect the displacement of the device against the wave period T1. The cycle between depth variations is similar, where in the sample t = 20 s to 30 s, there are around 8.25 displacement cycles. Thus, the displacement cycle frequency is 0.825 Hz while the sea wave frequency is 0.833 Hz. The displacement produced by the device shows a resonant movement characterized by the similarity of the sea wave frequency and the displacement cycle frequency.

However, there is a dissimilarity in the maximum displacement value at each depth variation. It was found that D2 produced the most significant displacement of 50.98°, followed by D1 at 26.12°, then D3 at 25.15°, and the smallest was D4 with a magnitude of around 15.39°. Depth variations also produced minimum values with the most significant values, namely D3 at around -16° followed by D4 at around -12° followed by D1 at around -10° and the smallest was D2 at around -8.7°. From the results of the maximum and minimum values, the water depth location affects significant environmental differences so that the maximum and minimum displacements are different, causing asymmetrical movements.

In the test with the specification of wave period T=1.6 s, each depth variation showed a similar displacement pattern over time, with an increase in the wave period significantly impacting the magnitude of displacement (see Figure 5). It was observed that the number of displacement cycles during this period decreased when compared to the previous wave period. In the period of 20 to 30 seconds, there were around 6.5 displacement cycles. The proportion of the maximum displacement value at each depth showed that D2 reached around 58°, followed by D3 at 33°, D1 at 16°, and D4 at 22°. Meanwhile, the minimum displacement value was recorded at D2 at -35°, followed by D1 at -31°, D3 at -28°, and D4 with a positive minimum value of 22°. Overall, the displacement pattern at various depths shifted towards the negative, especially at D3 and D4. This condition indicates that the device's movement is becoming more symmetrical compared to the response in the previous wave period.

Further testing was carried out with a wave period of T = 2 seconds, where the decrease in displacement cycles over time was increasingly evident (see Figure 6). Based on data from 20 to 30 seconds, each depth showed five cycles, which means a decrease of about 23% compared to the previous period. In addition, the change in device displacement increasingly tends to negative values, as seen from the minimum value at each depth, which decreases significantly along with the increase in the wave period. The maximum amplitude at depth D2 reached 78°, D1 was 3°, D3 was 39.5°, and D4 was 30.7°. Meanwhile, the minimum value recorded at D2 was -62°, D1 was -45°, D3 was -34°, and D4 was -27°. These results indicate that the increase in the wave period causes the movement of the device to be more symmetrical than the previous period, especially at depths D2, D3, and D4.

However, this does not apply to depth D1, where a shift in the displacement pattern is increasingly extreme in the negative direction. This phenomenon indicates that the device becomes less stable at shallower depths and tends to experience greater angular displacement in a particular direction.

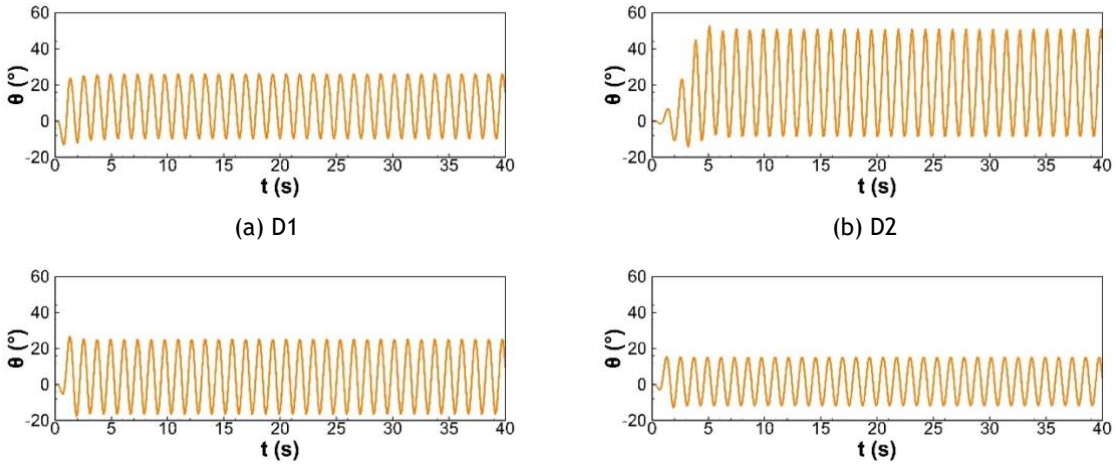


(a) D1 (b) D2

(c) D3 (d) D4

**Figure 4.** Comparison of displacement for each depth variation T=1.2 s.

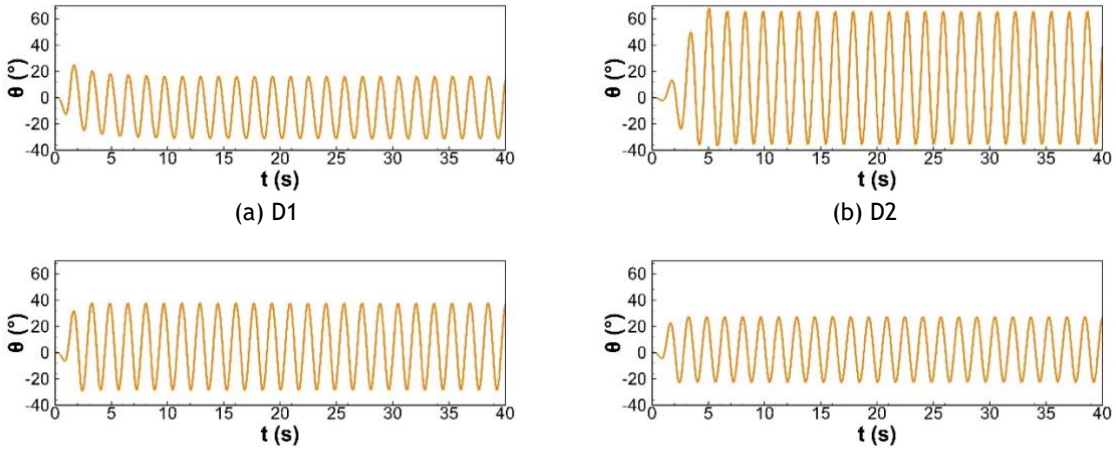


(a) D1 (b) D2

(c) D3 (d) D4

**Figure 5.** Comparison of displacement for each depth variation T=1.6 s.

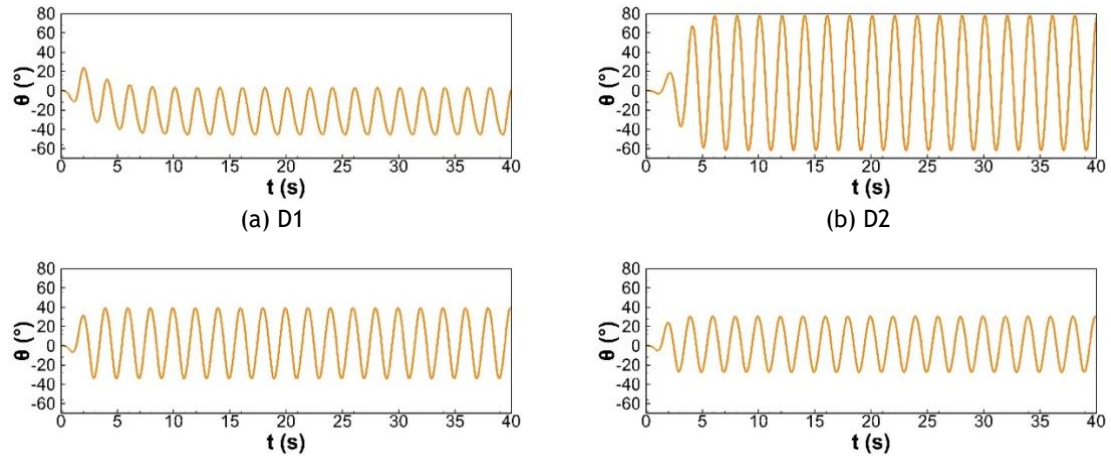


(a) D1 (b) D2

(c) D3 (d) D4

**Figure 6.** Comparison of displacement for each depth variation T=2 s.

In the test with a wave period of T = 2.4 seconds, as presented in Figure 7, the number of displacement cycles shows a further decrease compared to the previous period variations. In the time range of 20 to 30 seconds, there are only four cycles, indicating that increasing the wave period influences the oscillation frequency of the device. Again, the highest maximum amplitude is found at a depth of D2, around 75°, while the smallest amplitude occurs at a depth of D1 of 23°. At a depth of D4, the maximum amplitude is recorded at 29°, and D3, it is 36°. The minimum values of each depth show a similar pattern, with D2 reaching -67° and D1 at -51°. Based on these maximum and minimum value data, increasing the wave period further increases the symmetry of the flap movement at depths of D2, D3, and D4. However, this condition is not achieved at D1, where there is an increasingly extreme displacement shift towards the negative direction, showing that the stability and balance of the flap movement are still challenging to achieve at shallower depths. This indicates that a particular depth significantly affects the energy distribution, with an optimal depth such as D2 producing the most efficient and symmetric oscillations.

The variation of the last period with T = 2.8 second, as shown in Figure 8, shows that the displacement frequency per unit time is decreasing compared to the previous wave period. In the 20 to 30 seconds, only about 3.5 cycles were recorded, indicating that the higher the wave period, the frequency of the displacement cycle will decrease. The maximum amplitude was again recorded at a depth of D2 with a value of about 68°, while the smallest amplitude occurred at D4, which was 25°. A more symmetrical displacement oscillation pattern was visible at D2, D3, and D4 depths, indicating that an increase in the wave period contributed to an increase in the symmetry of the device's movement.

However, this condition did not occur at D1, where the displacement shifted significantly in the negative direction. This fact is consistent with the results in the previous period, where the depth of D1 produced a more extreme and less stable response. Thus, it can be concluded that the optimal depth, such as D2, increases the displacement amplitude and maintains the symmetry of the device's motion. In contrast, at shallow depths, such as D1, the device tends to experience imbalance, which reduces the overall motion efficiency.

From the overall displacement presented, the higher the sea wave period will affect the decrease in cycle intensity at each depth variation. This phenomenon happens because the frequency of sea waves will align with the frequency of the OWSC device displacement cycle. Thus, the greater the wave period, the less frequent the frequency of the sea waves. This phenomenon leads to a reduction in the number of device cycles as the sea wave period increases. This finding aligns with recent work by Liu, who demonstrated that more extended wave periods reduce the dynamic response and energy conversion efficiency of OWSC systems due to lower wave frequencies (Liu *et al.*, 2022).

Furthermore, the influence of water depth on the device can be analyzed through the maximum and minimum displacement values at each wave period. The highest maximum displacement value is produced by depth D2 at period T = 2 seconds, while the most minor displacement is recorded at depth D4 at period T = 1.2 seconds. The resultant force acting on the OWSC environmental system, including hydrostatic pressure, has been calculated using numerical calculations with the unit of pascal (Pa). So, the hydrostatic force is one of the parameters that play a role in the OWSC displacement. Hydrostatic pressure increases with increasing water depth, while wave energy tends to decrease. This fact explains why depth D2 has the highest maximum displacement value. This phenomenon is caused by the hydrostatic pressure received by the flap at depth D2, which is relatively minor compared to deeper depths.

In contrast, the wave energy received by the flap remains maximum at that depth, allowing the flap to move optimally without experiencing energy reduction due to excessive pressure. Similar results were highlighted by Zhang et al., who demonstrated that intermediate water depths optimize OWSC performance by maintaining sufficient wave energy while avoiding

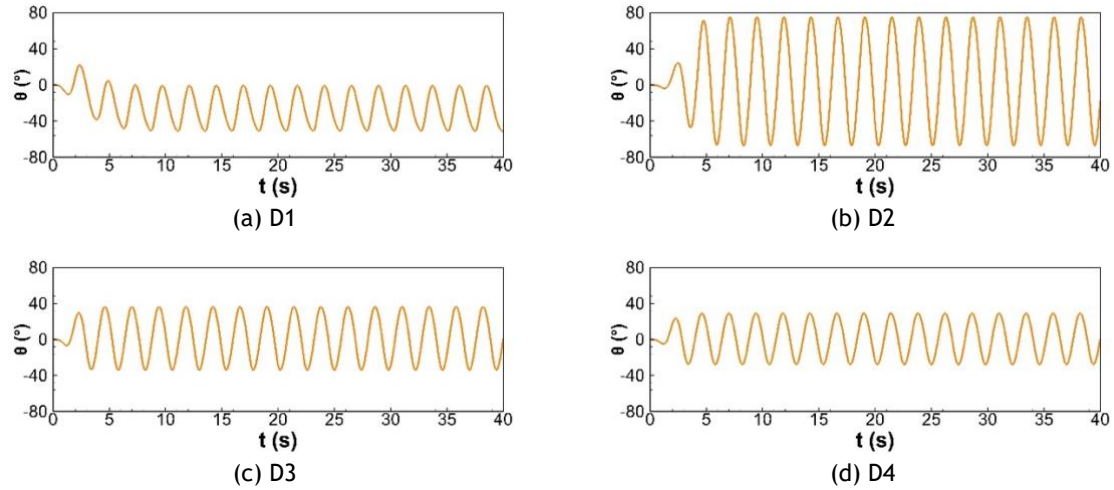


(a) D1 (b) D2

(c) D3 (d) D4

**Figure 7.** Comparison of displacement for each depth variation T=2.4 s.

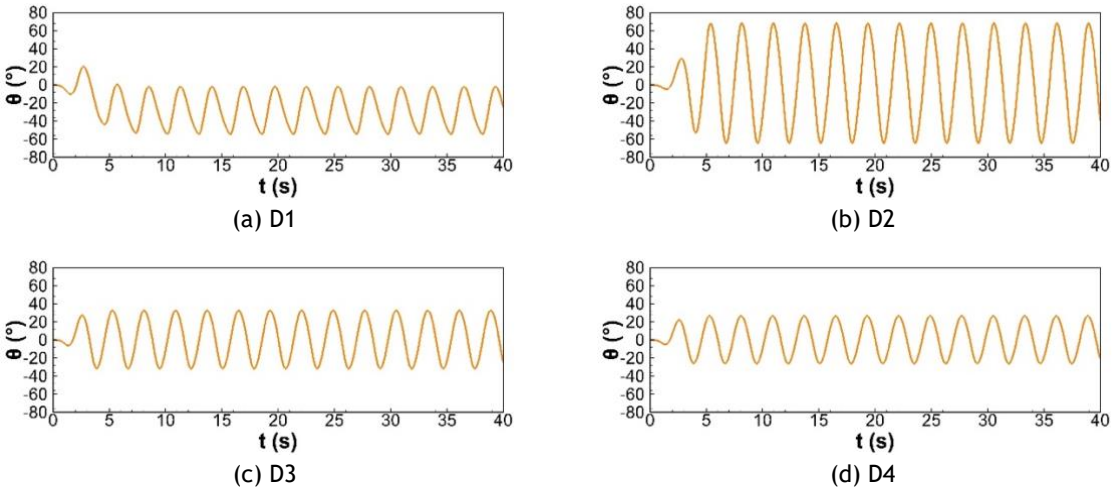


(a) D1 (b) D2

(c) D3 (d) D4

**Figure 8.** Comparison of displacement for each depth variation T=2.8 s.

excessive hydrostatic pressure (Zhang, Zhu and Cheng, 2023). Conversely, the most minor displacement at a depth of D4 is caused by increased hydrostatic pressure at a greater depth. High hydrostatic pressure at this depth reduces the amplitude of water wave oscillations because most of the wave energy is absorbed or damped before reaching the flap. As a result, the thrust received by the flap becomes smaller as hydrostatic increases, and the displacement of the device also decreases. This observation corroborates findings from Qu, showing that deep water significantly reduces wave energy transfer efficiency due to increased damping effects and wave dissipation (Qu *et al.*, 2022).

On the other hand, at shallower depths such as D1, low hydrostatic pressure causes wave energy to be more efficiently delivered to the device but tends to produce unstable movement due to the dominance of the pulling force in a specific direction, so the symmetry of the displacement is disturbed. This behavior aligns with observations made by Cheng, who noted that shallow water depths increase wave energy efficiency but introduce instability in OWSC movement due to irregular forces acting on the flap (Cheng *et al.*, 2020).

These results show that the optimal depth, such as D2, is in a condition of sufficient hydrostatic pressure to maximize wave energy conversion without experiencing excessive energy damping. The balance between hydrostatic pressure and wave energy at intermediate depths is consistent with recent findings by liu,

emphasizing that intermediate depths are optimal for OWSC devices, ensuring stable movement and maximum energy capture efficiency (Liu *et al.*, 2022).

## 4. CONCLUSION

In this study, variations in seawater depth play a crucial role in influencing the performance of Oscillating Wave Surge Converters (OWSC). The characteristics of flap displacement highlight the significant impact of water depth on device efficiency. At extreme depths, both shallow and deep, the displacement is minimal. This influence is because the wave energy either does not reach the flap effectively in deep water or the flap is not able to move efficiently in shallow water due to inadequate hydrostatic support. The optimal depth for OWSC performance is found to be at depth D2, where the water depth is roughly equal to the flap height. At this depth, the flap is able to move with maximum efficiency, as the hydrostatic pressure is sufficient to support its motion without substantially reducing wave energy.

In terms of wave periods, each variation in the water wave period leads to a uniform frequency at different water depths, though the frequency of displacement cycles increases as the wave period decreases. This fact means that shorter wave periods cause a higher frequency of displacement cycles, which can affect the system's overall efficiency. A critical observation is that the symmetry of the displacement cycle improves at optimal depths, such as D2, where the displacement is the greatest. This phenomenon occurs because the hydrostatic pressure at this depth helps in supporting flap movement optimally, while wave energy remains high enough for efficient conversion into mechanical energy.

On the contrary, deeper depths like D4 cause high hydrostatic pressure, which reduces the oscillation amplitude. Most of the wave energy is absorbed before reaching the flap, which diminishes its displacement and reduces the overall energy captured. This high pressure at greater depths can limit the energy conversion efficiency of the OWSC. The hydrostatic pressure is low at shallower depths, like D1, but the flap's cross-sectional area is smaller, absorbing less wave energy. Consequently, this leads to instability and asymmetry in the flap's movement, reducing efficiency.

Thus, the study emphasizes that intermediate depths, such as D2, are optimal for OWSC devices. These depths allow for a balance of sufficient hydrostatic pressure to support stable flap movement while maximizing wave energy capture without excessive damping. This observation aligns with recent findings in wave energy research, where intermediate water depths were highlighted as ideal for maximizing both stability and energy efficiency in OWSC systems.

## REFERENCES

Bertram, D.V. *et al.* (2020) 'A Systematic Approach For Selecting Suitable Wave Energy Converters For Potential Wave Energy Farm Sites', *Renewable and Sustainable Energy Reviews*, 132, p. 110011. Available at: https://doi.org/10.1016/j.rser.2020.110011.

Cheng, Y. *et al.* (2020) 'Fully Nonlinear Investigations On Performance Of An OWSC (Oscillating Wave Surge Converter) In 3D (Three-Dimensional) Open Water', *Energy*, 210, p. 118526. Available at: https://doi.org/10.1016/j.energy.2020.118526.

Cheng, Y. *et al.* (2021) 'Wave Energy Extraction For An Array Of Dual-Oscillating Wave Surge Converter With Different Layouts', *Applied Energy*, 292, p. 116899. Available at: https://doi.org/10.1016/j.apenergy.2021.116899

Constant, C. *et al.* (2021) 'Accelerating Ocean-Based Renewable Energy Educational Opportunities To Achieve A Clean Energy Future', *Progress in Energy*, 3(4), p. 042002. Available at: https://doi.org/10.1088/2516-1083/ac1509.

Cui, J., Chen, X. and Dai, S. (2023) 'Numerical Study On Dual Oscillating Wave Surge Converter With Different Cross-Section Shapes Using SPH Under Regular Waves', *Ocean Engineering*, 271, p. 113755. Available at: https://doi.org/10.1016/j.oceaneng.2023.113755

Garrison, T. and Ellis, R. (2022) *Oceanography: An Invitation to Marine Science*. USA. Cengage Learning. [Print].

Gunawardane, S.D.G.S.P., Folley, M. and Kankanamge, C.J. (2019) 'Analysis Of The Hydrodynamics Of Four Different Oscillating Wave Surge Converter Concepts', *Renewable Energy*, 130, pp. 843–852.

Available at: https://doi.org/10.1016/j.renene.2018.06.115.

Julian, J. *et al*. (2024) 'Study Of Hydrodynamic Characteristics In Oscillating Wave Surge Converter', *Jurnal Polimesin*, 22(2), pp. 158–164. Available at: https://doi.org/10.30811/jpl.v22i2.4715.

Liu, Y. *et al*. (2022) 'Nonlinear Hydrodynamic Analysis And Optimization Of Oscillating Wave Surge Converters Under Irregular Waves', *Ocean Engineering*, 250, p. 110888. Available at: https://doi.org/10.1016/j.oceaneng.2022.110888

Qu, K. *et al*. (2022) 'Numerical Study on Hydrodynamics of Submerged Permeable Breakwater under Impacts of Focused Wave Groups Using a Nonhydrostatic Wave Model', *Journal of Marine Science and Engineering*, 10(11), p. 1618. Available at: https://doi.org/10.3390/jmse10111618.

Rahman, M. (1995) *Water Waves: Relating Modern Theory to Advanced Engineering Applications*. USA. Clarendon Press. [Print].

Roache, P.J. (1994) 'Perspective: A Method for Uniform Reporting of Grid Refinement Studies', *Journal Fluids of Engineering*, 116(3), pp. 405–413. Available at: https://doi.org/doi.org/10.1115/1.2910291.

Toffoli, A. and Bitner-Gregersen, E.M. (2017) 'Types of Ocean Surface Waves, Wave Classification', in *Encyclopedia of Maritime and Offshore Engineering*. John Wiley & Sons, Ltd, pp. 1–8. Available at: https://doi.org/10.1002/9781118476406.emoe077.

Tongphong, W. *et al*. (2021) 'A Study On The Design And Performance Of Moduleraft Wave Energy Converter', *Renewable Energy*, 163, pp. 649–673. Available at: https://doi.org/10.1016/j.renene.2020.08.130.

Wei, Y. *et al*. (2016) 'Wave Interaction With An Oscillating Wave Surge Converter. Part II: Slamming', *Ocean Engineering*, 113, pp. 319–334. Available at: https://doi.org/10.1016/j.oceaneng.2015.12.041

Wilberforce, T. *et al*. (2019) 'Overview Of Ocean Power Technology', *Energy*, 175, pp. 165–181. Available at: https://doi.org/10.1016/j.energy.2019.03.068.

Zhang, Y., Zhu, W. and Cheng, X. (2023) 'Wave Power Extraction Of Flap-Type Wave Energy Converter Array Mounted At The Stepped Bottom Topography', *Renewable Energy*, 218, p. 119334. Available at: https://doi.org/10.1016/j.renene.2023.119334.